FINAL REPORT

Microwave Observations of Precipitation and the Atmosphere

Covering the Period
January 1, 2002 – November 30, 2003

Submitted by

David H. Staelin and Philip W. Rosenkranz

February 23, 2004

Massachusetts Institute of Technology
Research Laboratory of Electronics
Cambridge, Massachusetts 02139

Microwave Observations of Precipitation and the Atmosphere

ABSTRACT

This research effort had three elements devoted to improving satellite-derived passive microwave retrievals of precipitation rate: morphological rain-rate retrievals, warm rain retrievals, and extension of a study of geostationary satellite options.

The morphological precipitation-rate retrieval method uses for the first time the morphological character of the observed storm microwave spectra. The basic concept involves: 1) retrieval of point rainfall rates using current algorithms, 2) using spatial feature vectors of the observations over segmented multi-pixel storms to estimate the integrated rainfall rate for that storm (m^3s^{-1}), and 3) normalization of the point rain-rate retrievals to ensure consistency with the storm-wide retrieval. This work is ongoing, but two key steps have been completed: development of a segmentation algorithm for defining spatial regions corresponding to single storms for purposes of estimation, and reduction of some of the data from NAST-M that will be used to support this research going forward.

The warm rain retrieval method involved extension of Aqua/AIRS/AMSU/HSB algorithmic work on cloud water retrievals. The central concept involves the fact that passive microwave cloud water retrievals over ~0.4 mm are very likely associated with precipitation. Since glaciated precipitation is generally detected quite successfully using scattering signatures evident in the surface-blind 54- and 183-GHz bands, this new method complements the first by permitting precipitation retrievals of non-glaciated events. The method is most successful over ocean, but has detected non-glaciated convective cells over land, perhaps in their early formative stages. This work will require additional exploration and validation prior to publication.

Passive microwave instrument configurations for use in geostationary orbit were studied. They employ parabolic reflectors between 2 and 4 meters in diameter, and frequencies up to ~430 GHz; this corresponds to nadir spot diameters as small as 10 km.

FINAL REPORT

Microwave Observations of Precipitation and the Atmosphere

I.   Introduction

This research program extended work completed under NASA Grants NAG5-10, NAG5-2545, and NAG5-7487, all of which were directed toward different aspects of passive microwave remote sensing of the terrestrial atmosphere from space. These efforts have been paralleled by separately funded but related MIT efforts directed toward improved definition and utilization of passive microwave imaging spectrometers on research aircraft (NAST), operational meteorological satellites (NOAA-15, -16, and -17), and research spacecraft (Aqua, geosynchronous microwave sounders).

This program had four principal elements devoted to improving satellite-derived passive microwave retrievals of precipitation rate: 1) morphological retrievals, 2) warm rain retrievals, 3) studies of geostationary satellite options, and 4) radiative transfer in scattering atmospheres; these are discussed below in Sections II-V, respectively.

II.   Storm-wide Precipitation-Rate Retrievals using the Millimeter-wave Bands

NAST-M passive microwave images obtained over convective storms clearly show that the apparent cell size increases markedly with observing frequency, suggesting that the spectral morphology of storms could contain additional information about precipitation rate. The physical basis for this supposition is that storm-wide precipitation is proportional to absolute humidity times vertical velocity times the effective area of the convective column ("effective" can be defined so as to make this relation exact). Since larger air-mass convection rates (vertical velocity x area x density) will convey larger ice particles to larger radial distances from convective cores before those hydrometeors fall down into the non-radially moving air masses below, the radial distance ice particles travel before falling into stagnant air increases with total convected air mass and therefore with total storm precipitation ($m^3 s^{-1}$).

Shear winds aloft tend to displace the center of the radially expanding outflow rather than increasing its extent, unless those winds are quite strong. Examples of radial flow behavior observed by NAST-M near Miami, Florida on July 13, 2002 are shown below in Figure 1. These cells reached altitudes over 12 km and the smallest ice particles were strongly displaced toward the west, as evidenced in the 425-GHz image. The larger particles fell out sooner and were displaced less.

Thus the area traversed by the larger ice particles before they fall out is a function of particle size and is related to the air mass outflow and integrated precipitation under

the glaciated cell top. Although one might hope the same method would apply to infrared observations as well, infrared responds too strongly to particles that fall too slowly to provide a reliable indicator of total convected air mass. In contrast, microwaves are sensitive only to ice particles heavy enough to fall sufficiently fast that their radial progress from the convective core is often usefully related to storm intensity. This microwave information can then supplement other microwave precipitation-rate retrieval information to provide improved retrieval performance.
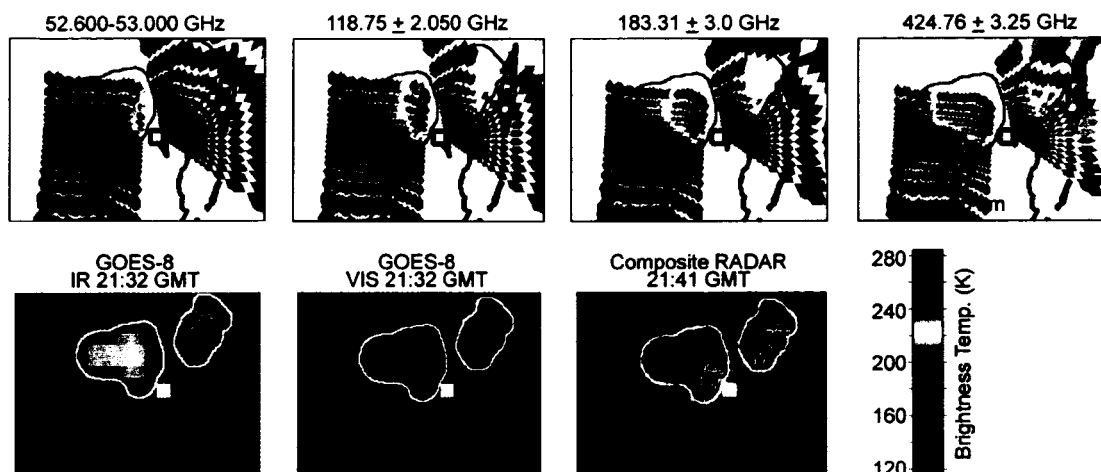

Figure 1. NAST-M brightness temperature observations of strong convective cells near 52.8, 118.7±2, 180.3±3, and 424.8±3.25 GHz, and associated images from radar and GOES-8 IR and visible channels.

These satellite and spacecraft microwave observations and the development of a physical model linking storm-wide precipitation rates to microwave signatures are being separately funded. Essential to testing these concepts, however, is a robust method for segmenting precipitation events observed by satellite into macro-cells for which such storm-wide retrievals can be performed. Figure 2(a) illustrates a typical precipitation rate retrieval image obtained by AMSU-A/B flying on the NOAA-15 satellite.[1] Figure 2(b) illustrates the automated decomposition of this image into macro-cells for regional retrieval purposes. This automated segmentation work constitutes part of the ongoing MS thesis of Jessica Loparo and part of this research program. The algorithm defines regions in terms of local maxima for which the highest saddle point between that maximum and any other local maximum is less than some fraction of the lesser of the two maxima. The boundaries between two regions are generally local minima lying on lines connecting two adjacent local maxima.

Under separate funding feature vectors characterizing these regions are being developed and will be used to generate storm-wide precipitation rate retrievals to be

---

[1] Chen and Staelin, TGARS, February 2003.

compared with simultaneous NEXRAD precipitation-rate retrievals integrated over the same set of segmented regions. The single-pixel precipitation-rate retrievals will then be normalized so as to be consistent with the corresponding storm-wide retrieval.
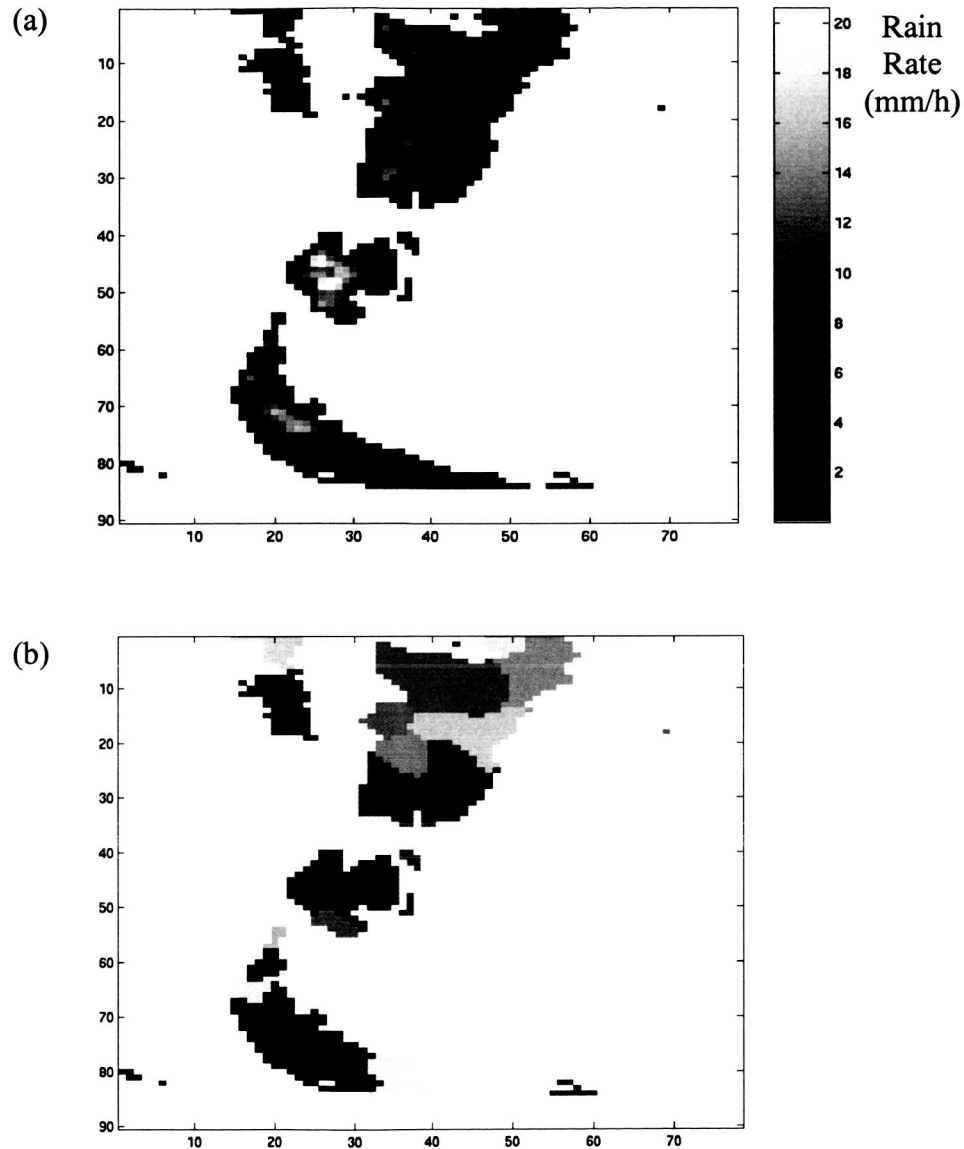

Figure 2. (a) Precipitation-rate retrievals obtained from NOAA-15 AMSU-A/B data using the method of Chen and Staelin[1]; (b) automatically segmented storm regions for which storm-wide retrievals will be obtained.

III. Warm Rain Retrievals

Current algorithms for retrieving rain rate using opaque microwave channel information[1] rely primarily on the strong scattering signatures of cold ice particles (e.g. graupel), and

therefore are much less sensitive to unglaciated precipitation or warm rain. As part of the NASA AIRS/AMSU/HSB program retrieval methods were developed to retrieve cloud liquid water altitude profiles over land and sea. These methods utilize the fact that the relative humidity generally does not exceed 100 percent, and excessive values of retrieved absorption in the retrieved humidity profile are therefore probably due to cloud water.

The current program has been examining whether these retrieved cloud water profiles can be used for precipitation retrievals of unglaciated precipitation. Although most storms are sufficiently glaciated to preclude cloud water profile retrievals, there are some exceptions. Figure 3 shows a rain-rate scatterplot of an extended storm over the North Atlantic on September 6, 2002. The rain rate inferred from the glaciated signature is well correlated with the maximum cloud water density retrieved anywhere in the associated column of air. The triggering density inferred from this figure is ~0.02 g m^{-3}, and the average rain rate appears to be linearly proportional to peak cloud water density as that density increases above the 0.02 g m^{-3} threshold. The peak density appears to be more predictive of precipitation rate than column-integrated water. This is plausible on physical grounds because the altitude extent of warm rain varies
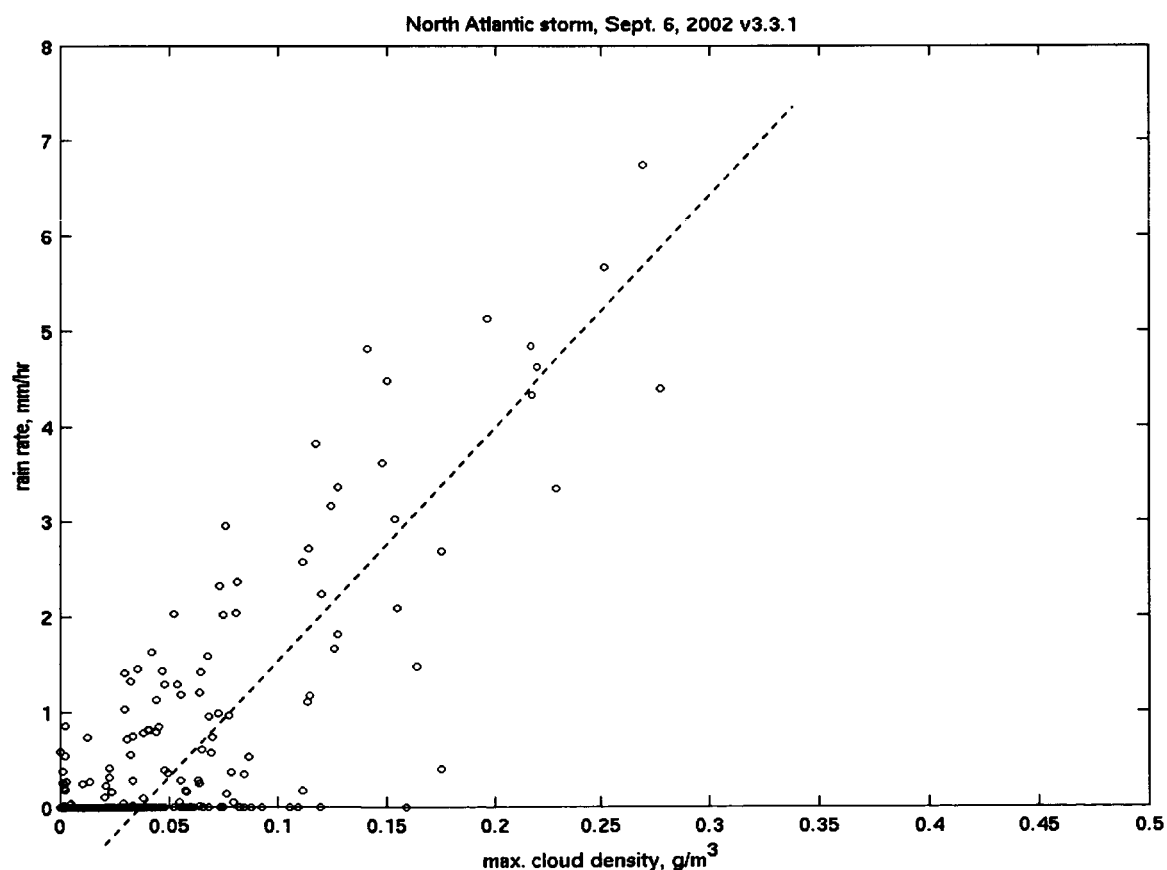

Figure 3. Inferred rain rate versus retrieved maximum cloud water density

Figure 4 shows images that superimpose rain rate retrievals based on glaciated signatures (yellow/red scale) with images of retrieved integrated cloud liquid water (blue/green scale), where levels above ~0.5 mm are likely to be warm rain. This data was obtained with AIRS/AMSU/HSB on Aqua on September 6, 2002. The tendency of the liquid water retrievals to lie below 0.25 or above 0.5 mm suggests that precipitation may be initiated somewhere between these two limits.
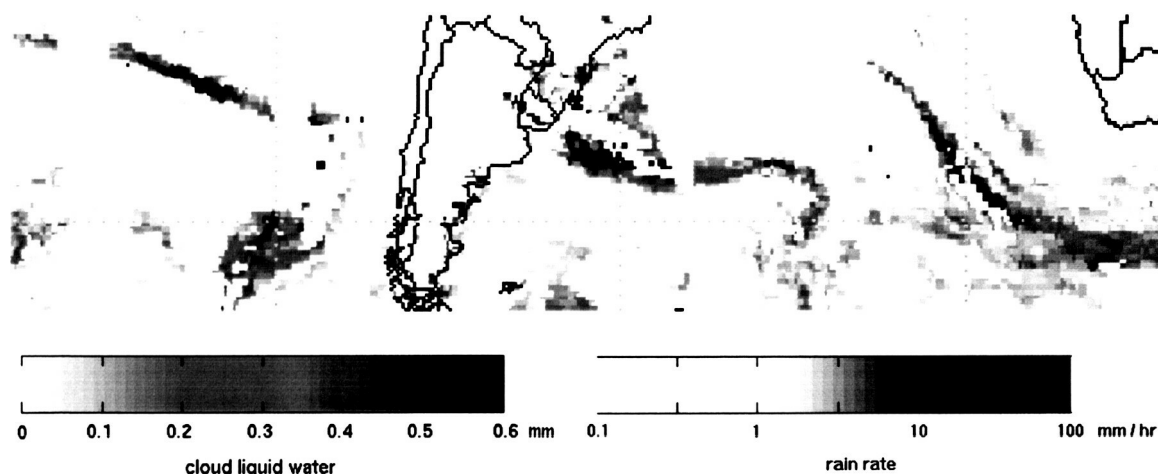

Figure 4. Retrievals of glaciated rain and of non-glaciated rain (over 0.5 mm water)

The potential importance of this new method for retrieving precipitation rate lies partly in that it appears to work over both land and sea because of its inclusion of the opaque channels. For example, see the thin band of warm rain retrieved at the southern end of the glaciated rain over northern Argentina.

IV.   Geostationary Satellite Options

Passive microwave instrument configurations for use in geostationary orbit were studied further. The configurations considered employ parabolic reflectors between 2 and 4 meters in diameter, and frequencies up to ~430 GHz; this corresponds to nadir spot diameters as small as 10 km. The work described in Section II above is particularly relevant to this opportunity because storm-wide retrievals would require less spatial resolution and would permit use of higher frequencies with improved spatial resolution, thus offering two types of improvement over geosynchronous systems employing lower frequencies (degrading spatial resolution) and viewing smaller targets (storm signatures over land are spatially smaller at lower opaque frequencies). Two papers on this subject are cited in the references below.

REFERENCES:

Chen, F.W. and D.H. Staelin, "AIRS/AMSU/HSB Precipitation Estimates," *IEEE Transactions on Geoscience and Remote Sensing, 41*, 2, pp 410-417, 2003.

Bizzarri, B., A.J. Gasiewski, and D.H. Staelin, "Initiative for MW/mm sounding from geostationary orbit," IEEE International Geoscience and Remote Sensing Symposium, Toronto, Canada, Vol. 1, pp 548-552, June 24-28, 2002.

Gasiweski, A.J., D.H. Staelin, and B. Bizzarri, "The Geosynchronous Microwave Sounder Imager," Twelfth International TOVS Study Conference, Lorne, Australia, February 27-March 5, 2002.